Smooth connectivity in real algebraic varieties

Joseph Cummings * Jonathan D. Hauenstein † Hoon Hong‡ Clifford D. Smyth§

September 26, 2024

Abstract

A standard question in real algebraic geometry is to compute the number of connected components of a real algebraic variety in affine space. This manuscript provides algorithms for computing the number of connected components, the Euler characteristic, and deciding the connectivity between two points for a smooth manifold arising as the complement of a real hypersurface of a real algebraic variety. When considering the complement of the set of singular points of a real algebraic variety, this yields an approach for determining smooth connectivity in a real algebraic variety. The method is based upon gradient ascent/descent paths on the real algebraic variety inspired by a method proposed by Hong, Rohal, Safey El Din, and Schost for complements of real hypersurfaces. Several examples are included to demonstrate the approach.
Keywords. Connectivity, smooth points, real algebraic sets, polynomial systems, homotopy continuation, numerical algebraic geometry

1 Introduction

In real affine space $\mathbb{R}^n$, a real algebraic variety has the form

$$X = V_{\mathbb{R}}(g_1, \ldots, g_k) = \{x \in \mathbb{R}^n \mid g_1(x) = \cdots = g_k(x) = 0\} \tag{1}$$

where $g_1, \ldots, g_k \in \mathbb{R}[x_1, \ldots, x_n]$, that is, polynomials in $x = (x_1, \ldots, x_n)$ with real coefficients. Many problems in science and engineering can be translated into questions regarding real algebraic varieties. For example, the real algebraic variety X could describe the configuration space of a mechanism and path planning (e.g., see [6, 13, 16]) corresponds with determining connected paths between two points on X. Moreover, singularity-free path planning (e.g., see [10, 11]) corresponds with determining smooth connections between two points on X. Due to its ubiquity, there are many algorithms proposed for deciding connectivity with a non-exhaustive list being [3,5,14,15,17–19,27].

The approach in [20, 21] considers connectivity in $\mathbb{R}^n \backslash V_{\mathbb{R}}(f)$, where $f \in \mathbb{R}[x_1, \ldots, x_n]$, using connections between critical points via gradient ascent paths. The algorithms described below are based on this work, but generalized to consider $X_f = X \backslash V_{\mathbb{R}}(f)$ which is assumed to be smooth.

*Department of Applied and Computational Mathematics and Statistics, University of Notre Dame, Notre Dame, IN 46556 (jcummin7@nd.edu)

†Department of Applied and Computational Mathematics and Statistics, University of Notre Dame, Notre Dame, IN 46556 (hauenstein@nd.edu, https://www.nd.edu/~jhauenst)

‡Department of Mathematics, North Carolina State University, Raleigh, NC 27695 (hong@ncsu.edu, https://hong.math.ncsu.edu/)

§Department of Mathematics and Statistics, University of North Carolina at Greensboro, Greensboro, NC 27402 (cdsmyth@uncg.edu, https://sites.google.com/view/cliffordsmyth/)

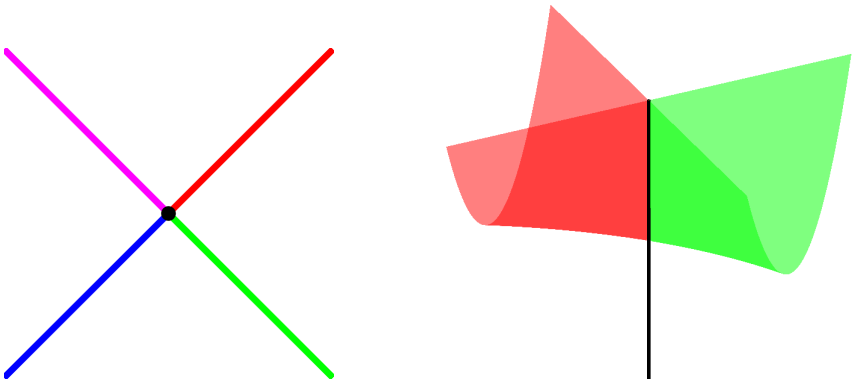

(a) (b)

Figure 1: (a) Four smoothly connected components for a pair of intersecting lines with the singular point at the intersection. (b) Two smoothly connected components for the Whitney umbrella with the singular points forming the "handle" of the umbrella.

That is, $X \cap V_{\mathbb{R}}(f)$ is assumed to at least contain the singular points of X. Thus, connected components of X_f are smoothly connected in X. For example, Figure 1(a) shows that the pair of intersecting lines $V_{\mathbb{R}}(x_1^2 - x_2^2)$ has four smoothly connected components using $f = 4(x_1^2 + x_2^2)$ while Figure 1(b) shows that the Whitney umbrella $V_{\mathbb{R}}(x_1^2 - x_2^2 x_3)$ has two smoothly connected components using $f = 4x_1^2 + 4x_2^2 x_3^2 + x_2^4$. Additionally, given a point in X_f, one can decide which smoothly connected component the point belongs to yielding an approach to decide if two points lie on the same smoothly connected component.

The rest of the paper is organized as follows. Section 2 provides a summary of preliminary topics. Section 3 describes routing functions which are the basis for the algorithms in Section 4. Section 5 proves the correctness of the algorithms while Section 6 demonstrates the algorithms on some examples. A short conclusion is provided in Section 7.

2 Preliminaries

The following summarizes some background information that will be used throughout.

2.1 Smooth points

The following provides a short summary of smooth points with more details found in, e.g., [4]. For X as in (1), the dimension of X, denoted $\dim X$, is the largest d such that $(0,1)^d$ injects by a semi-algebraic map into X. If $\dim X = d$, a point $x \in X$ is a smooth point of X, if there is an open neighborhood of x in X which is a d-dimensional submanifold, i.e., the tangent space of x with respect to X, denoted $T_x X$, is d-dimensional. A point $x \in X$ is a singular point of X if it is not a smooth point. Let X_{reg} and X_{sing} be the set of smooth and singular points of X, respectively. Hence, $X = X_{\text{reg}} \cup X_{\text{sing}}$ and $X_{\text{reg}} \cap X_{\text{sing}} = \varnothing$, i.e., $X_{\text{reg}} = X \backslash X_{\text{sing}}$.

Example 2.1. *For $X = V_{\mathbb{R}}(x_1^2 - x_2^2)$ as in Figure 1(a),* $\dim X = 1$ *and* $X_{\text{sing}} = V_{\mathbb{R}}(x_1, x_2) = \{(0,0)\}$. *For $X = V_{\mathbb{R}}(x_1^2 - x_2^2 x_3)$ as in Figure 1(b),* $\dim X = 2$ *and* $X_{\text{sing}} = V_{\mathbb{R}}(x_1, x_2) = \{(0,0,x_3) \mid x_3 \in \mathbb{R}\}$, *called the "handle" of the Whitney umbrella.*

The following will be assumed throughout which relates the smooth points with respect to X with the null space of the Jacobian matrix of the defining polynomials $g_1, \ldots, g_k$.

Assumption 2.2. *For X as in (1), let $g = \{g_1, \ldots, g_k\}$ and $Jg(x)$ be the $k \times n$ Jacobian matrix of g at x. Then, it is assumed that the system g is such that the following holds:*

$$X_{\text{reg}} = \{x \in X \mid \dim \operatorname{null} Jg(x) = \dim X\}.$$

For $m = n - \dim X$, let M_m be the set of $m \times m$ minors of $Jg(x)$ and $S = \sum_{p \in M_m} p^2$. Therefore,

$$X_{\text{sing}} = X \cap V_{\mathbb{R}}(M_m) = X \cap V_{\mathbb{R}}(S) = V_{\mathbb{R}}(g_1, \ldots, g_k, S) \quad \text{and} \quad X_{\text{reg}} = X \backslash V_{\mathbb{R}}(S).$$

For example, Assumption 2.2 can always be satisfied by replacing $g_1, \ldots, g_k$ with a generating set for the real radical, e.g., see [9], of the ideal $\langle g_1, \ldots, g_k \rangle$. This assumption, which provides that the tangent space of X at $x \in X_{\text{reg}}$ corresponds with the null space of $Jg(x)$, is utilized when proving Theorem 3.4.

Example 2.3. *For $X = V_{\mathbb{R}}(x_1^2 - x_2^2)$, $g = x_1^2 - x_2^2$ satisfies Assumption 2.2 with $n = 2$ and $\dim X = 1$. Moreover, $M_1 = \{2x_1, -2x_2\}$ with $S = 4(x_1^2 + x_2^2)$ yields*

$$X_{\text{sing}} = X \cap V_{\mathbb{R}}(M_1) = X \cap V_{\mathbb{R}}(S) = V_{\mathbb{R}}(x_1, x_2).$$

For $X = V_{\mathbb{R}}(x_1^2 - x_2^2 x_3)$, $g = x_1^2 - x_2^2 x_3$ satisfies Assumption 2.2 with $n = 3$ and $\dim X = 2$. Moreover, $M_1 = \{2x_1, -2x_2 x_3, -x_2^2\}$ with $S = 4x_1^2 + 4x_2^2 x_3^2 + x_2^4$ yields

$$X_{\text{sing}} = X \cap V_{\mathbb{R}}(M_1) = X \cap V_{\mathbb{R}}(S) = V_{\mathbb{R}}(x_1, x_2).$$

In particular, $\{x_1, x_2\}$ is a generating set for the real radical of $\langle g, S \rangle$ in both of these cases.

A semi-algebraic connected set $C \subset X$ is said to be smoothly connected if $C \subset X_{\text{reg}}$. Moreover, the smoothly connected components of X are the connected components of X_{reg}.

Example 2.4. *For $X = V_{\mathbb{R}}(x_1^2 - x_2^2)$, the smoothly connected components are*

$$C_1 = \{(t,t) \mid t > 0)\},\ C_2 = \{(t,-t) \mid t > 0\},\ C_3 = \{(-t,t) \mid t > 0\}, \text{ and } C_4 = \{(-t,-t) \mid t > 0\}$$

as illustrated in Figure 1(a). For $X = V_{\mathbb{R}}(x_1^2 - x_2^2 x_3)$, the smoothly connected components are

$$C_1 = \{(uv, u, v^2) \mid u > 0, v \in \mathbb{R}\} \text{ and } C_2 = \{(uv, u, v^2) \mid u < 0, v \in \mathbb{R}\}$$

as illustrated in Figure 1(b).

2.2 Gradient system

Let X be as in (1) which satisfies Assumption 2.2. Suppose that $a, b \in \mathbb{R}[x_1, \ldots, x_n]$ such that $X \cap V_{\mathbb{R}}(b) = \varnothing$ and $f = a/b$. Hence, f is a rational function defined everywhere on X with $V_{\mathbb{R}}(f) = V_{\mathbb{R}}(a)$. Moreover, suppose that

$$X \backslash V_{\mathbb{R}}(f) \subset X_{\text{reg}} \quad \text{and, equivalently,} \quad X_{\text{sing}} \subset X \cap V_{\mathbb{R}}(f). \tag{2}$$

Let $X_f = X \backslash V_{\mathbb{R}}(f) \subset X_{\text{reg}}$. Since X_f is a manifold, the gradient of f on X_f, denoted $\nabla_{X_f} f$, is well-defined. Note that $f \neq 0$ on X_f so the connected components of X_f are the union of the

connected components of $X_f \cap \{f > 0\}$ and $X_f \cap \{f < 0\}$. Thus, one can perform gradient ascent on X_f when starting at a point with $f > 0$ and gradient descent on X_f when starting at a point with $f < 0$ and remain in X_f. In particular, suppose that $x_0 \in X_f$ and $\sigma_0 = \operatorname{sign} f(x_0) \in \{-1, +1\}$, then the gradient system under consideration is formally written as

$$\begin{array}{rcll} \dot{x}(t) & = & \sigma_0 \cdot \nabla_{X_f} f(x) & \text{on } X_f \\ x(0) & = & x_0. & \end{array} \tag{3}$$

Of course, gradient systems on manifolds are well-studied, e.g., [24, 29]. Computationally, one can consider (3) using a local tangential parameterization. Suppose that $d = \dim X$ and $x \in X_f$. Let $V_x \in \mathbb{R}^{n \times d}$ be an orthogonal matrix such that its columns form an orthonormal basis for $T_x X_f$. Hence, $Jg(x)V_x = 0$ and $V_x^T V_x = I_d$, the $d \times d$ identity matrix. Let $\pi_x : X_f \to \mathbb{R}^d$ such that $\pi_x(y) = V_x^T(y - x)$ is the orthogonal projection from X_f to $T_x X_f$ centered at x (see Figure 2), i.e., $\pi_x(x) = 0$. Since $x \in X_f \subset X_{\text{reg}}$, there exists $\epsilon_x > 0$ such that π_x restricted to $X_f \cap B_{\epsilon_x}(x)$ is invertible, where

$$B_{\epsilon_x}(x) = \{y \in \mathbb{R}^n \mid \|y - x\| < \epsilon_x\} \quad \text{with} \quad \|y - x\| = \sqrt{(y_1 - x_1)^2 + \cdots + (y_n - x_n)^2}.$$

Since $U_x = \pi_x(X_f \cap B_{\epsilon_x}(x)) \subset \mathbb{R}^d$ is an open neighborhood of the origin, (3) can be considered locally in parameterizing coordinates $p \in U_x$ with $y(p) = \pi^{-1}(p) \in X_f \cap B_{\epsilon_x}(x)$. In particular,

$$\nabla_{X_f} f(x) = \nabla_{\mathbb{R}^n} f(x) \cdot V_x \in \mathbb{R}^d. \tag{4}$$

Moreover, the corresponding Hessian matrix is

$$H_{X_f} f(x) = \sum_{i=1}^{n} \frac{\partial f}{\partial x_i}(x) \cdot W_x^i + V_x^T \cdot H_{\mathbb{R}^n} f(x) \cdot V_x \in \mathbb{R}^{d \times d}$$

where $W_x^1, \ldots, W_x^n \in \mathbb{R}^{d \times d}$ are symmetric and form the unique solution to the linear system

$$\begin{aligned} \sum_{i=1}^{n} \frac{\partial g_j}{\partial x_i}(x) \cdot W_x^i + V_x^T \cdot H_{\mathbb{R}^n} g_j(x) \cdot V_x &= 0 \quad \text{for } j = 1, \ldots, k, \\ \sum_{i=1}^{n} (V_x)_{ij} \cdot W_x^i &= 0 \quad \text{for } j = 1, \ldots, d. \end{aligned}$$

In particular,

$$y(p) = x + V_x \cdot p + \frac{1}{2} \begin{bmatrix} p^T \cdot W_x^1 \cdot p \\ \vdots \\ p^T \cdot W_x^n \cdot p \end{bmatrix} + \text{higher order terms} \tag{5}$$

such that $g(y(p)) = 0$ since $y(p) \in X_f$.

Example 2.5. *For $X = V_{\mathbb{R}}(x_1^2 - x_2^2)$ and $f = 4(x_1^2 + x_2^2)$, let $x = (1, 1)$ so that*

- $V_x = \frac{1}{\sqrt{2}} \begin{bmatrix} 1 \\ 1 \end{bmatrix}$, $W_x^1 = [0]$, $W_x^2 = [0]$;
- $\nabla_{X_f} f(x) = \nabla_{\mathbb{R}^2} f(x) \cdot V_x = 8\sqrt{2}$;
- $H_{X_f} f(x) = \frac{\partial f}{\partial x_1}(x) \cdot W_x^1 + \frac{\partial f}{\partial x_2}(x) \cdot W_x^2 + V_x^T \cdot H_{\mathbb{R}^2} f(x) \cdot V_x = 8$.

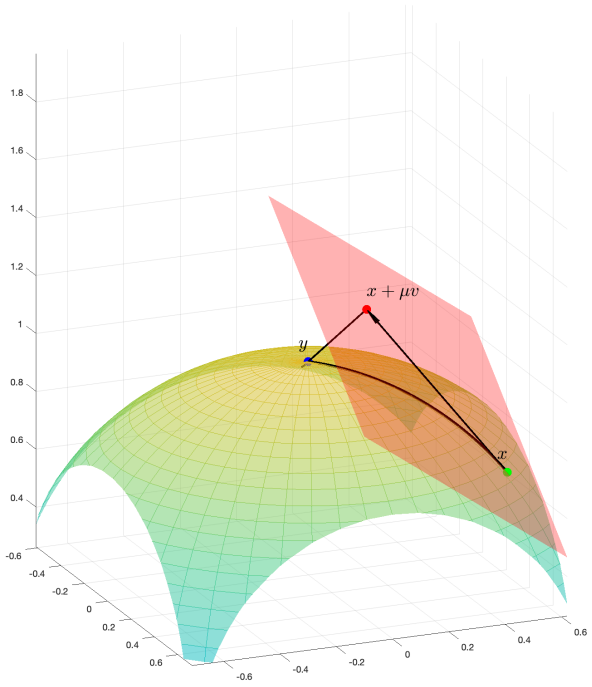

Figure 2: An example of a tangential parameterization of X centered at x. The green point is x, the red point is $p = x + \mu v$ for $v \in T_x X$, and the blue point is $y = \pi_x^{-1}(p)$.

Since X is locally linear at x, $y(p) = x + V_x \cdot p$ for $p \in \mathbb{R}$. Hence, for $q(p) = f(y(p))$, one has $\nabla_{\mathbb{R}} q(0) = \nabla_{X_f} f(1,1)$ and $H_{\mathbb{R}} q(0) = H_{X_f} f(1,1)$.

Similarly, for $X = V_{\mathbb{R}}(x_1^2 - x_2^2 x_3)$ and $f = 4x_1^2 + 4x_2^2 x_3^2 + x_2^4$, let $x = (1,1,1)$ so that

- $V_x = \frac{1}{\sqrt{2}} \begin{bmatrix} 1 & 1/3 \\ 1 & -1/3 \\ 0 & 4/3 \end{bmatrix}$, $W_x^1 = \begin{bmatrix} 0 & 4/27 \\ 4/27 & -16/81 \end{bmatrix}$, $W_x^2 = -W_x^1$, $W_x^3 = -W_x^1/2$;
- $\nabla_{X_f} f(x) = \nabla_{\mathbb{R}^3} f(x) \cdot V_x = \frac{2\sqrt{2}}{3} \begin{bmatrix} 15 & 7 \end{bmatrix}$;
- $H_{X_f} f(x) = \frac{\partial f}{\partial x_1}(x) \cdot W_x^1 + \frac{\partial f}{\partial x_2}(x) \cdot W_x^2 + \frac{\partial f}{\partial x_3}(x) \cdot W_x^3 + V_x^T \cdot H_{\mathbb{R}^3} f(x) \cdot V_x = \frac{2}{81} \begin{bmatrix} 567 & 303 \\ 303 & 127 \end{bmatrix}$.

For $y(p)$ as in (5) and $q(p) = f(y(p))$, then $\nabla_{\mathbb{R}^2} q(0) = \nabla_{X_f} f(1,1,1)$ and $H_{\mathbb{R}^2} q(0) = H_{X_f} f(1,1,1)$.

3 Routing points and routing functions

The keys to the algorithms in [20,21] are routing points and routing functions. Suppose that X as in (1) satisfies Assumption 2.2 and let $r : X \to \mathbb{R}$ be a twice continuously differentiable function on X such that $r(x) = 0$ for all $x \in X_{\text{sing}}$, i.e., $X_r = X \backslash V_{\mathbb{R}}(r) \subset X_{\text{reg}}$. A point $z \in X$ is called a *routing point* of r on X if $z \in X_r$, i.e., $r(z) \neq 0$, and $\nabla_{X_r} r(z) = 0$, which is equivalent to

$$\dim \operatorname{null} \begin{bmatrix} \nabla_{\mathbb{R}^n} r(z)^T & \nabla_{\mathbb{R}^n} g_1(z)^T & \cdots & \nabla_{\mathbb{R}^n} g_k(z)^T \end{bmatrix} = \dim X. \tag{6}$$

One can formulate (6) using [7] which, when $k = n - \dim X$, is equivalent to using Lagrange multipliers. Moreover, a routing point z is *nondegenerate* if $H_{X_r} r(z)$ is invertible. Since the gradient system (3) depends upon a sign, the index of a nondegenerate routing point is also sign dependent. In particular, the *index* of a nondegenerate routing point z is the number of eigenvalues of $H_{X_r} r(z)$ of the same sign as $r(z)$. Eigenvectors of $H_{X_r} r(z)$ corresponding with the eigenvalues of the same sign as $r(z)$ are called *unstable eigenvector directions*. For example, if $r(z) > 0$, then, since (3) is aiming to increase the function value, the index is the dimension of the local ascending manifold at z, which is the number of positive eigenvalues of $H_{X_r} r(z)$, and the eigenvectors corresponding with a positive eigenvalue are the unstable eigenvector directions.

Definition 3.1. *The function r is called a* routing function *on X if the following conditions hold:*

1. $X_r = X \backslash V_{\mathbb{R}}(r) \subset X_{\mathrm{reg}}$,
2. *for all $\epsilon > 0$, there exists $\delta > 0$ such that if $x \in X$ with $\|x\| \geqslant \delta$, then $|r(x)| \leqslant \epsilon$,*
3. *the corresponding set of routing points on X is finite and each is nondegenerate,*
4. *for each $\alpha \in \mathbb{R}\backslash\{0\}$, there is at most one routing point x on X satisfying $r(x) = \alpha$, and*
5. *the norms of r, $\nabla_{X_r} r$, and $H_{X_r} r$ are bounded on X_r.*

In particular, a routing function vanishes on X_{sing} as well as at infinity, and each level set contains at most one routing point. Therefore, if C is a connected component of X_r, then r on C must obtain either a minimum (if $r < 0$ on C) or a maximum (if $r > 0$ on C), which must occur at a routing point. The following formalizes this.

Proposition 3.2. *With the assumptions and definitions above, there is at least one routing point in each connected component of X_r of index 0.*

Example 3.3. *For $X = V_{\mathbb{R}}(x_1^2 - x_2^2)$, the function $f(x) = 4(x_1^2 + x_2^2)$ is not a routing function on X since f is unbounded on X. Nonetheless, consider the following rational function related to f:*

$$r(x) = \frac{4(x_1^2 + x_2^2)}{((x_1 - 1/2)^2 + (x_2 - 1/3)^2 + 1)^2}, \tag{7}$$

so that $X_r = X_f$. In fact, r is a routing function with four routing points $(\pm 7/(6\sqrt{2}), \pm 7/(6\sqrt{2}))$. Proposition 3.2 holds with exactly one routing point in each connected component of X_r as illustrated in Figure 3, with each being a local maximum of r along X_r. Thus, each routing point has index 0. The colors in Figure 3 verifies that r takes different values at each of the routing points.

The following provides a generalization of the construction used in Example 3.3 to create a routing function derived from [20, 21].

Theorem 3.4. *Suppose that X as in (1) satisfies Assumption 2.2 and $f \in \mathbb{R}[x_1, \ldots, x_n]$ such that $X_f = X \backslash V_{\mathbb{R}}(f) \subset X_{\mathrm{reg}}$. Let $\ell \in \mathbb{Z}_{>0}$ such that $2\ell > \deg f$. Then, there is a Zariski open dense subset $\mathcal{U} \subset \mathbb{R}^n$ such that, for every $c \in \mathcal{U}$,*

$$r_c(x) = \frac{f(x)}{((x_1 - c_1)^2 + \cdots + (x_n - c_n)^2 + 1)^\ell}$$

is a routing function on X.

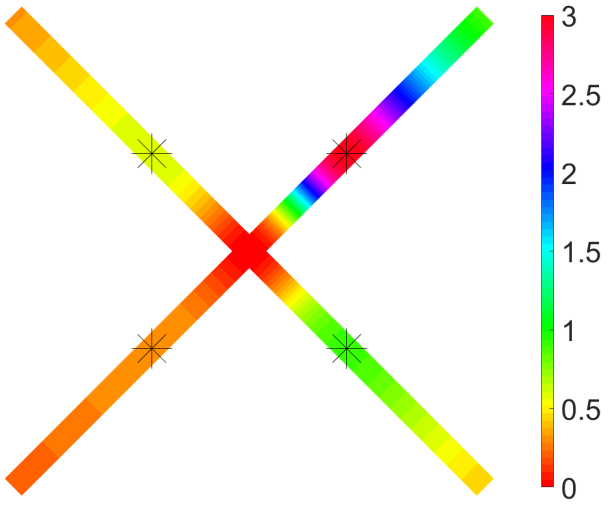

Figure 3: Pair of intersecting lines colored based on the value of the routing function with the four routing points marked, each corresponding to a local maxima of the routing function.

Proof. Let $c \in \mathbb{R}^n$ and define $D_c(x) = (x_1 - c_1)^2 + \cdots + (x_n - c_n)^2 + 1$. Thus, $r_c(x) = f(x) \cdot D_c(x)^{-\ell}$. Since D_c does not vanish on $\mathbb{R}^n$, r_c is infinitely differentiable with $X_{r_c} = X_f \subset X_{\text{reg}}$. Moreover, $2\ell > \deg f$ ensures that r_c is bounded on $\mathbb{R}^n$ (and hence on X) and vanishes at infinity. Additionally,

$$\nabla_{\mathbb{R}^n} r_c(x) = \nabla_{\mathbb{R}^n} f(x) \cdot D_c(x)^{-\ell} - 2 \cdot \ell \cdot f(x) \cdot D_c(x)^{-\ell-1} \cdot (x - c) \tag{8}$$

is also bounded on $\mathbb{R}^n$ for the same reason. Since V_x in (4) is orthonormal, this shows that $\nabla_{X_{r_c}} r_c$ is bounded on X. A similar argument shows that $H_{X_{r_c}} r_c$ is also bounded on X_{r_c} since the matrices W_x^j describe the local curvature of $X_f \subset X_{\text{reg}}$ and V_x is orthonormal.

All that remains is showing that the set of routing points is finite, each is nondegenerate, and evaluate to different values of r_c for values c in a Zariski open dense subset of $\mathbb{R}^n$. Since f and D_c are nonzero on X_{r_c}, (6) can be equivalently formulated as

$$\dim \operatorname{null} \begin{bmatrix} \frac{1}{2\cdot\ell} \cdot \frac{\nabla_{\mathbb{R}^n} f(x)^T}{f(x)} - \frac{(x-c)}{D_c(x)} & \nabla_{\mathbb{R}^n} g_1(x)^T & \cdots & \nabla_{\mathbb{R}^n} g_k(x)^T \end{bmatrix} = \dim X.$$

Note that the last k columns have a null space dimension equal to $\dim X$ on $X_{r_c} = X_f \subset X_{\text{reg}}$ via Assumption 2.2 and are independent of c. Moreover, the first column has the term $\frac{x-c}{D_c(x)}$ that is independent of f and g. Hence, the routing points of r_c on X_f correspond with the points in X_f where the first column is contained in the span of the last k columns. As c is varied, this aforementioned term forces the location of the routing points of r_c on X_{r_c} to change. Since this term is in the gradient of r_c, this also forces the value of r_c to instantaneously change as well. Therefore, the remaining part now follows from an algebraic version of Sard's theorem, e.g., see [28, Thm. A.4.10], as in the proof of [21, Thm. 36].

□

Theorem 3.4 shows that one can obtain a routing function using a generic $c \in \mathbb{R}^n$.

Example 3.5. *To demonstrate a value of c that does not work, consider $X = V_{\mathbb{R}}(x_1^2 + x_2^2 - 1)$ with $f = 4(x_1^2 + x_2^2)$. For $\ell = 2$, consider $c = 0$ so that $r_0(x)$ is as in (7). With this, every point on X*

is a critical point so that r_0 is not a routing function on X. However, with $c = (1/2, 1/3)$, then

$$r_c(x) = \frac{4(x_1^2 + x_2^2)}{((x_1 - 1/2)^2 + (x_2 - 1/3)^2 + 1)^2}$$

is a routing function with two routing points: $(3/\sqrt{13}, 2/\sqrt{13})$ is a maximum (index 0) and its antipodal point $(-3/\sqrt{13}, -2/\sqrt{13})$ is a minimum (index 1) of r_c on X.

Example 3.6. *For $X = V_{\mathbb{R}}(x_1^2 - x_2^2 x_3)$, consider $f(x) = 4x_1^2 + 4x_2^2 x_3^2 + x_2^4$ from Example 2.3. Consider $c \in \mathbb{R}^3$ and $\ell = 3$ so that*

$$r_c(x) = \frac{4x_1^2 + 4x_2^2 x_3^2 + x_2^4}{((x_1 - c_1)^2 + (x_2 - c_2)^2 + (x_3 - c_3)^2 + 1)^3}.$$

When $c = 0$, then r_0 is not a routing function since the two routing points $(0, \pm\sqrt{2}, 0)$ are degenerate, i.e., $H_{X_r} r$ is not invertible at these two points. With, say $c = (1/2, 1/3, 1/4)$, then r_c is a routing function with six routing points: 4 local maxima and 2 saddles with index 1. This is considered again in Example 4.3 with routing points on the Whitney umbrella shown in Figure 5.

Example 3.7. *For $X = V_{\mathbb{R}}(x_1^2 - x_2^2 x_3)$, consider $f(x) = x_1 x_2 x_3$ which means that X_f is the set of all points in X where all three coordinates are nonzero. The function*

$$r_0(x) = \frac{x_1 x_2 x_3}{(x_1^2 + x_2^2 + x_3^2 + 1)^2}$$

is not a routing function since two pairs of routing points are in the same level set. However, as suggested by the proof of Theorem 3.4, perturbing away from being centered at the origin destroys the symmetric structure so that, say $c = (1/6, 1/5, 1/4)$, yields a routing function, namely

$$r_c(x) = \frac{x_1 x_2 x_3}{((x_1 - 1/6)^2 + (x_2 - 1/5)^2 + (x_3 - 1/4)^2 + 1)^2}. \tag{9}$$

This yields four routing points, two are local maxima with $r_c > 0$ and two are local minima with $r_c < 0$ as shown in Figure 4. With the sign dependent notion of index, all four have index 0.

For a routing function r on X, the Euler characteristic of X_r is determined by counting the number of routing points of each index as summarized in the following.

Theorem 3.8. *When r is a routing function for X as in (1) which satisfies Assumption 2.2, then the Euler characteristic of X_r is*

$$\chi(X_r) = \sum_{j=0}^{d} (-1)^j \mathrm{rk}_j^{X_r} \tag{10}$$

where $\mathrm{rk}_j^{X_r}$ is the number of routing points of r on X_r of index j.

Proof. Let $C_1, \ldots, C_s$ be the connected components of X_r. Since the Euler characteristic is additive, it is enough to prove the formula on each connected component.

Suppose that C is a connected component of X_r and let $z_1, \ldots, z_k$ be the routing points of r contained in C. Since r has the same sign on C, we will consider the positive and negative cases separately. Suppose that $r > 0$ on C and let $0 < \delta < \min\{r(z_1), \ldots, r(z_k)\}$. Thus, r is a Morse function on C corresponding to the gradient vector field $\nabla_{X_r} r$ and we can retract C to

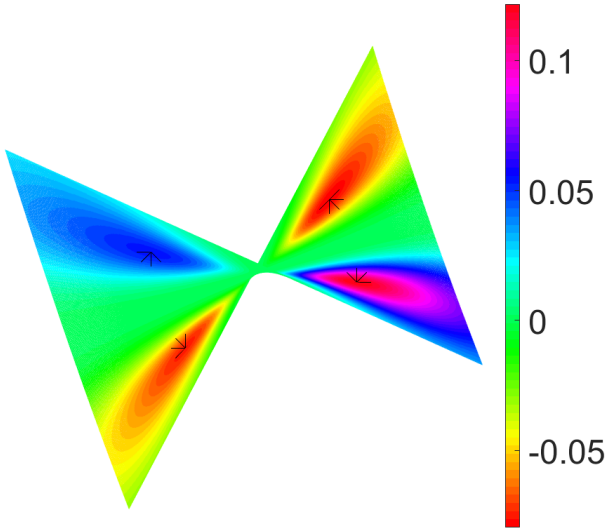

Figure 4: Whitney umbrella with coordinate axes removed and four routing points marked, each corresponding to a local optima of r_c as in (9).

$C_\delta = (r|_C)^{-1}([\delta, \infty))$ via the vector field, where $r|_C$ is the restriction of r to C. Since C_δ is a smooth compact manifold with boundary as $r|_C$ is bounded, it is well-known, e.g. [26, §2.3], that

$$\chi(C_\delta) = \sum_{j=0}^{d} (-1)^j \mathrm{rk}_j^C$$

where rk_j^C is the number of routing points in C of index j (corresponding to positive eigenvalues). As the Euler characteristic is invariant under homotopy, $\chi(C) = \chi(C_\delta)$ as claimed.

Similarly, if $r < 0$ on C, let $\max\{r(z_1), \ldots, r(z_k)\} < \delta < 0$. Thus, r is a Morse function on C corresponding to the gradient vector field $-\nabla_{X_r} r$ and we can retract C to $C_\delta = (r|_C)^{-1}((-\infty, \delta])$ via the vector field. The same formula holds with index corresponding to negative eigenvalues. □

Example 3.9. *For Example 3.3, the corresponding Euler characteristic is* $(-1)^0 \cdot 4 = 4$. *Additionally, the Euler characteristic of the unit circle is* $(-1)^0 \cdot 1 + (-1)^1 \cdot 1 = 0$ *from Example 3.5. From Example 3.6, the Euler characteristic of the Whitney umbrella with the "handle" removed is* $(-1)^0 \cdot 4 + (-1)^1 \cdot 2 = 2$. *Finally, the Euler characteristic of the Whitney umbrella with the coordinate axes removed is* $(-1)^0 \cdot 4 = 4$ *from Example 3.7.*

4 Connectivity algorithms

The number of connected components of $X_r = X_f$ is bounded above by the number of routing points of r on X_r of index 0 via Proposition 3.2. The following shows how to partition the set of routing points into subsets precisely corresponding to the connected components using the gradient system (3). The key to this computation is tracking from routing points with positive index. Since a routing point is a stationary point of (3), for routing points of positive index, one needs to consider (3) in an instantaneous initial direction in order to have non-stationary trajectory. By adapting the approach of [20, 21], this yields a connectivity algorithm. Thus, this gradient

representation of smoothly connected components via a routing function and routing points provides an analog to witness sets for complex irreducible varieties which permit membership testing, e.g., see [28, Chap. 13-15].

To set the stage, first consider an initial point which is not a routing point.

Proposition 4.1. *Suppose that X in* (1) *satisfies Assumption 2.2 and r is a routing function on X. If $x_0 \in X_r$ is not a routing point, i.e., $\nabla_{X_r} r(x_0) \neq 0$, then* (3) *defines a unique trajectory which limits to a routing point of r on X_r.*

Proof. Recall that for a routing function, r, $\nabla_{X_r} r$, and $H_{X_r} r$ are all bounded on X_r and hence, for any $a > 0$, $X_r \cap r^{-1}((-\infty, -a] \cup [a, \infty))$ is compact. Standard existence and uniqueness theory for initial value problems, e.g., [22, § 8.1, Thm. 3], adapted to manifolds shows that (3) has a unique solution $x(t) \in X_r$ for all $t \geqslant 0$. Moreover, since x_0 is not a routing point, $r(x(t))$ is strictly monotonic while $x(t)$ must be bounded. Hence, $z = \lim_{t\to\infty} x(t)$ is well-defined with $|r(z)| > |r(x_0)| > 0$. Boundedness also implies that one must have $\nabla_{X_r} r(z) = 0$, i.e., the trajectory limits to a routing point. □

Proposition 4.1 together with stationary trajectories starting at routing points shows that the gradient vector field on X_r defined by $\operatorname{sign}(r(x)) \cdot \nabla_{X_r} r(x)$ is complete. Numerically, trajectories which limit to an index 0 routing point are robust and the limit point is the corresponding steady-state solution computed via time marching using a numerical differential equation solver. Conversely, trajectories which limit to a routing point of positive index are numerically unstable as arbitrarily small numerical perturbations theoretically change the corresponding limit. However, from a numerical perspective, the proof in Section 5 shows that the key to computing a correct decomposition is accurately computing limits of trajectories when they limit to an index 0 routing point. For trajectories not limiting to an index 0 routing point, all that is needed from a numerical perspective is to compute another routing point in the same smoothly connected component where the value of $|r|$ has increased, which is easily accomplished by having $|r|$ be monotonically increasing along numerically approximated trajectories.

Next, consider an initial point which is a routing point $z \in X_r$ with an initial direction $v \in \mathbb{R}^n$ in the tangent space of X_r at z with $\|v\| = 1$ Since z is nondegenerate, there exists $\epsilon_0 > 0$ such that z is the unique routing point in $X_r \cap B_{\epsilon_0}(z)$ and the orthogonal projection from X_r to $T_z X_r$ centered at z is invertible. Thus, for $\epsilon \in (0, \epsilon_0)$, one can apply Proposition 4.1 with initial condition $x_0 = \pi^{-1}(z + \epsilon \cdot v)$ to yield trajectory $x_\epsilon(t)$. By uniqueness, $\lim_{\epsilon\to 0^+} x_\epsilon(t)$ is well-defined and limits to a routing point of r on X_r. This is summarized in the following.

Proposition 4.2. *Suppose that X in* (1) *satisfies Assumption 2.2 and r is a routing function on X. Suppose that $z \in X_r$ is a routing point and $v \in \mathbb{R}^n$ is a unit vector in the tangent space of X_r at z. Letting $x_\epsilon(t)$ be the trajectory from Proposition 4.1 starting at the orthogonal projection of $z + \epsilon \cdot v$ onto X_r, then $x(t) = \lim_{\epsilon\to 0^+} x_\epsilon(t)$ is well-defined trajectory which limits to a routing point of r on X_r.*

Example 4.3. *To illustrate Propositions 4.1 and 4.2, consider Example 3.6 with $c = (1/2, 1/3, 1/4)$. First, consider the trajectory emanating from the non-routing point $x_0 = (-2.25, 1.5, 2.25)$ which limits to a routing point that is a local maximum. In Figure 5, x_0 is shown in red with the trajectory (yellow) limiting to a routing point (black). Second, consider the trajectories emanating from the index 1 saddle points, approximately $(-0.5002, 1.0635, 0.2212)$ and $(-0.5255, -1.3526, 0.1509)$, in the two directions arising from the unstable eigenvector. In Figure 5, each of these two trajectories are shown (green and magenta) which limit to a routing point that is a local maximum.*

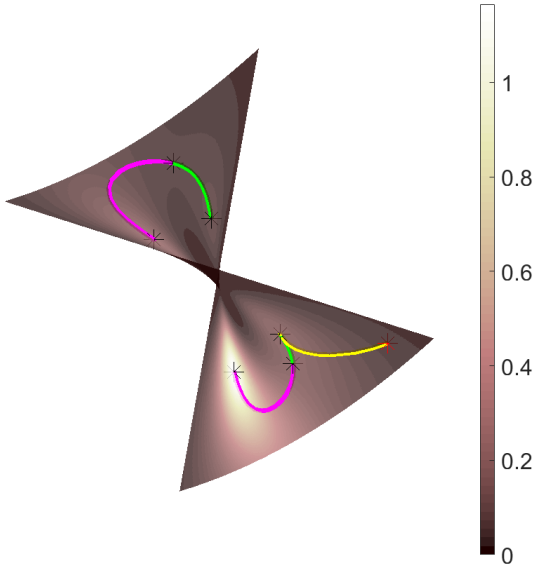

Figure 5: Whitney umbrella with "handle" removed and six routing points marked (black). Illustration of a trajectory (yellow) from a non-routing point (red) along with two trajectories (green and magenta) emanating from each index 1 saddle in the unstable eigenvector direction which connects the local maxima on the same connected component.

As observed in Figure 5, the trajectories from the saddles in an unstable eigenvector direction connect the local optima that lie in the same connected component. This holds in general and is summarized in Algorithm 1 and Theorem 4.4.

The matrix A in Algorithm 1 is constructed to be reflexive (diagonal entries are 1) and symmetric. Thus, transitive closure means to enforce the transitivity property, i.e., if z_i is connected to z_j which is connected to z_k, then z_i is connected to z_k. Using Boolean matrix multiplication and addition, the transitive closure of $A \in \mathbb{R}^{m\times m}$ is

$$M = A + A^2 + \cdots + A^m.$$

In particular, $M_{ij} = 1$ if and only if z_i and z_j lie on the same connected component of X_r.

Algorithm 2 uses the output of Algorithm 1 as input to answer connectivity queries.

Theorem 4.4. *Algorithms 1 and 2 are correct.*

A proof is presented in Section 5.

Example 4.5. *From Example 4.3, one can write the matrices A and M in Algorithm 1 as*

$$A = \begin{bmatrix} 1 & 0 & 1 & 0 & 0 & 0 \\ 0 & 1 & 1 & 0 & 0 & 0 \\ 1 & 1 & 1 & 0 & 0 & 0 \\ 0 & 0 & 0 & 1 & 0 & 1 \\ 0 & 0 & 0 & 0 & 1 & 1 \\ 0 & 0 & 0 & 1 & 1 & 1 \end{bmatrix} \quad \textit{and} \quad M = \begin{bmatrix} 1 & 1 & 1 & 0 & 0 & 0 \\ 1 & 1 & 1 & 0 & 0 & 0 \\ 1 & 1 & 1 & 0 & 0 & 0 \\ 0 & 0 & 0 & 1 & 1 & 1 \\ 0 & 0 & 0 & 1 & 1 & 1 \\ 0 & 0 & 0 & 1 & 1 & 1 \end{bmatrix}.$$

That is, M shows that X_r has two connected components each corresponding with three routing points, two local maxima and a saddle of index 1 as illustrated in Figure 5. Thus, since $X_r = X_{\text{reg}}$ where X is the Whitney umbrella, the Whitney umbrella has two smoothly connected components.

Input: Polynomials $g_1, \ldots, g_k \in \mathbb{R}[x_1, \ldots, x_n]$ with $X = V_{\mathbb{R}}(g_1, \ldots, g_k)$ satisfying Assumption 2.2 and routing function r.
Output: Euler characteristic of X_r and partitioned subset of the routing points of r on X_r corresponding to the connected components of X_r.
Computing the routing points of r on X_r, say $z_1, \ldots, z_m$, and corresponding indices, say $i_1, \ldots, i_m$.
Compute $\chi = \sum_{j=1}^{m} (-1)^{i_j}$.
Initialize $A = I_m$, the $m \times m$ identity matrix.
for $j = 1, \ldots, m$ **do**
  foreach *unstable eigenvector* v *for* $H_{X_r} r(z_j)$ **do**
    Compute limit routing point from z_j in the direction v with respect to r, say z_{w_+}.
    Set $A_{jw_+} = A_{w_+ j} = 1$.
    Compute limit routing point from z_j in the direction $-v$ with respect to r, say z_{w_-}.
    Set $A_{jw_-} = A_{w_- j} = 1$.
  end
end
Set M to be the transitive closure of A.
Partition $\{z_1, \ldots, z_m\}$ based on the connected components of M, say $C_1, \ldots, C_s$.
return $(\chi, \{C_1, \ldots, C_s\})$

Algorithm 1: Euler characteristic and connected components

Input: Polynomials $g_1, \ldots, g_k \in \mathbb{R}[x_1, \ldots, x_n]$ with $X = V_{\mathbb{R}}(g_1, \ldots, g_k)$ satisfying Assumption 2.2, routing function r, partitioned subsets $C_1, \ldots, C_s$ of the routing points of r on X_r corresponding to the connected components of X_r, and points $p, q \in X_r$.
Output: $True$ if p and q lie on the same connected component of X_r and $False$ otherwise.
if p *is a routing point* **then**
  Set $p' \in \{1, \ldots, s\}$ so that $p \in C_{p'}$.
else
  Compute limit routing point z_{j_p} via Proposition 4.1 starting at p.
  Set $p' \in \{1, \ldots, s\}$ so that $z_{j_p} \in C_{p'}$.
end
if q *is a routing point* **then**
  Set $q' \in \{1, \ldots, s\}$ so that $q \in C_{q'}$.
else
  Compute limit routing point z_{j_q} via Proposition 4.1 starting at q.
  Set $q' \in \{1, \ldots, s\}$ so that $z_{j_q} \in C_{q'}$.
end
return $True$ *if* $p' = q'$, *else* $False$

Algorithm 2: Connectivity query

Example 4.6. *From Example 3.7, the Whitney umbrella with the coordinate axes removed decomposes into four connected components.*

5 Correctness proof

The following presents a proof of Theorem 4.4. Clearly, the Euler characteristic follows from Theorem 3.8. The correctness of Algorithm 2 follows from the statement and proof of Proposition 4.1 with strict monotonicity showing p and z_{j_p} as well as q and z_{j_q} lie on the same connected component of X_r. In particular, Algorithm 2 depends upon correct input computed via Algorithm 1. Now, in Algorithm 1, Proposition 4.2 yields that routing point z_j is connected to routing points z_{w+} and z_{w-}. Since the transitive closure ensures the transitivity of the connections described by A, the only thing left to show regarding Algorithm 1 is that the connections derived from unstable eigenvectors suffice for determining the connected components via the mountain pass theorem.

For a routing point z, the stable manifold of z with respect to r on X_r is

$$M_r(z) = \{z\} \cup \{x_0 \in X_r \mid \nabla_{X_r} r(x_0) \neq 0 \text{ and the trajectory from Proposition 4.1 limits to } z\}.$$

The proof of [2, Thm 4.2] can be trivially adapted to this case with appropriate adjustments to conclude that $\operatorname{codim} M_r(z)$ is the index of z with respect to r, e.g., if z is a routing point with $r(z) > 0$ and is a local maximum (index 0), then $\dim M_r(z) = \dim X_r$. Clearly, uniqueness of trajectories yields

$$X_r = \bigsqcup_{\text{routing points } z} M_r(z).$$

Therefore, for a connected component C of X_r, one has

$$C = \bigsqcup_{\text{routing points } z \in C} M_r(z). \tag{11}$$

In this way, one is identifying each connected component with the finitely many routing points that lie inside of it.

Suppose that $z_0 \in C$ is a routing point. If $\dim M_r(z_0) < \dim X_r$, i.e., the index of z_0 is positive, then select any unstable eigenvector direction and let z_1 be the corresponding routing point as in Proposition 4.2. Hence, $z_1 \in C$ and $|r(z_0)| < |r(z_1)|$. If $\dim M_r(z_1) < \dim X_r$, one can repeat this process yielding a sequence of routing points $z_0, z_1, \ldots$ with $|r(z_j)| < |r(z_{j+1})|$. Hence, this must be a sequence of distinct routing points. Since there are only finitely many routing points, this process must terminate after finitely many steps yielding, say, a routing point $z_\ell \in C$ with $\dim M_r(z_\ell) = \dim X_r$, i.e., the index of z_ℓ is 0. Therefore, this shows that every routing point in C is connected to some routing point of index 0 in C by trajectories following unstable eigenvector directions. Hence, all that remains is showing connectivity between routing points of index 0 in C.

For a routing point z, let $\overline{M_r(z)}$ denote the Euclidean closure of $M_r(z)$ in X_r. Since

$$\bigsqcup_{\text{index} > 0 \text{ routing points } z \in C} M_r(z)$$

has positive codimension, it immediately follows that

$$C = \bigcup_{\text{index 0 routing points } z \in C} \overline{M_r(z)}.$$

Suppose that z and z' are distinct routing points in C of index 0 with $S_{z,z'} = \overline{M_r(z)} \cap \overline{M_r(z')} \neq \varnothing$. Such a pair must exist when C contains at least two index 0 routing points by connectivity of C.

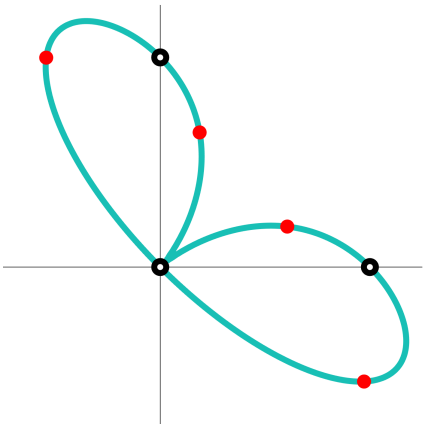

Figure 6: Four routing points for a quartic curve away from the coordinate axes

Hence, $r(z) \neq r(z')$. Since r vanishes at infinity, for any $\alpha \neq 0$, $V_{\mathbb{R}}(r-\alpha)$ is compact. Thus, r satisfies the Palais-Smale condition and the Mountain Pass Theorem [1] (see also [25, Thm. 3]) shows the existence of an index 1 routing point z'' in $S_{z,z'}$ so that z and z' are connected by trajectories emanating from the unstable eigenvector direction at z''.

Since C is connected and there are only finitely many routing points, one can repeat this argument to create a sequence of connecting trajectories between any two index 0 routing points in C. Therefore, Algorithm 1 correctly identifies the connected components of X_r.

6 Examples

The following considers various examples for computing smoothly connected components. The routing points were computed using `Bertini` [8] and the trajectories were computed using `Matlab`.

6.1 Positive solutions

In order to compute the number of smoothly connected components in the positive orthant, one can choose a routing function r so that $X_r \subset (\mathbb{R}^*)^n$ where $\mathbb{R}^* = \mathbb{R}\backslash\{0\}$ and then only consider routing points in the positive orthant. For example, one can reconsider both Example 3.3 and Example 3.7 to see that each has a single routing point in the positive orthant, i.e., each has one smoothly connected component in the positive orthant.

For another example, consider the compact quartic curve $X \subset \mathbb{R}^2$ from [12, Ex. 9] defined by

$$g(x) = x_1^4 + x_2^4 - (x_1 - x_2)^2(x_1 + x_2) = 0.$$

Since $X \cap (\mathbb{R}^*)^2 \subset X_{\text{reg}}$, one can consider the routing function

$$r(x) = \frac{x_1 x_2}{((x_1 - 1/3)^2 + (x_2 - 1/2)^2 + 1)^2}.$$

This yields four routing points as shown in Figure 6. Two of the routing points have a negative coordinate and are ignored. This leaves two routing points with positive coordinates, each of which is a local maximum yielding that $X \cap (\mathbb{R}_{>0})^2$ has two smoothly connected components.

Surface	# index 0	# index 1	# index 2	χ	# smoothly connected components
Dingdong	2	2	1	1	2
Calypso	2	2	0	0	2
Chubs	32	44	4	-8	8
Twilight	2	1	1	2	2
Eistute	7	4	1	4	4
Seepferdchen	7	11	2	-2	1

Table 1: Summary data for some algebraic surfaces in $\mathbb{R}^3$

6.2 Some surfaces

With the Whitney umbrella used as an illustrative example, the following summarizes computing the Euler characteristic and the number of smoothly connected components for the following surfaces in $\mathbb{R}^3$:[1]

- (Dingdong) $g(x) = x_1^2 + x_2^2 - x_3^2 + x_3^3$
- (Calypso) $g(x) = x_1^2 + x_2^2 x_3 - x_3^2$
- (Chubs) $g(x) = x_1^4 + x_2^4 + x_3^4 - (x_1^2 + x_2^2 + x_3^2) + 1/2$
- (Twilight) $g(x) = (x_1^2 + x_2^2 - 3)^3 + (x_3^3 - 2)^2$
- (Eistute) $g(x) = (x_1^2 + x_2^2)^3 - 4x_1^2 x_2^2 (x_3^2 + 1)$
- (Seepferdchen) $g(x) = x_1^4 - 5x_1^2 x_2^3/2 + x_2^6 - (x_1 + x_2^2)x_3^3$

Table 1 summarizes the results of the computations when taking $f(x) = \|\nabla_{\mathbb{R}^3} g(x)\|^2$ and

$$r(x) = \frac{f(x)}{((x_1 - c_1)^2 + (x_2 - c_2)^2 + (x_3 - c_3)^2 + 1)^{\deg g}} \quad \text{where} \quad c = \begin{bmatrix} 0.7978234324 \\ 0.6623073432 \\ 0.2347907832 \end{bmatrix}$$

in which c was selected randomly.

6.3 Connectivity in real projective space

In [23, Ex. 6.4], for small $\epsilon > 0$, the following octic curve in $\mathbb{P}^4_{\mathbb{R}}$ is shown to consist of six ovals:

$$\begin{bmatrix} (x_2 + x_3)(x_2 + x_3 - x_4) + \epsilon(x_1^2 + 2x_1 x_3 - x_1 x_4 + x_3^2 - x_3 x_4) + \epsilon^2 x_0^2 \\ x_0(x_2 + x_3 - x_4) + \epsilon(x_0 x_3 - x_0 x_4 + x_1 x_3 - x_1 x_4 + x_2 x_4 + x_3 x_4 - x_4^2) - \epsilon^2 x_4^2 \\ x_0(x_1 + x_3) + \epsilon(x_0 x_4 + x_1 x_2 + x_1 x_3 + x_1 x_4 + x_2 x_3 - x_2 x_4 + x_3^2) \end{bmatrix} = 0.$$

To verify this, fix $\epsilon = 10^{-2}$, and consider the double cover on the unit sphere in $\mathbb{R}^5$ by appending $x_0^2 + \cdots + x_4^2 - 1$ to the system above yielding a smooth compact degree 16 curve $X \subset \mathbb{R}^5$. Since X is smooth and compact with $X \cap V(x_4) = \varnothing$, we can use the routing function $r(x) = x_4$ with $X = X_r$. This yields 40 routing points which arise as 20 pairs of antipodal points. Thus, one only

[1] See `https://homepage.univie.ac.at/herwig.hauser/bildergalerie/gallery.html`, `https://silviana.org/gallery/hauser/`, and `https://www-sop.inria.fr/galaad/surface/` for additional information.

needs to consider the 20 routing points with $x_4 > 0$ which arise as 10 local maxima (index 0) and 10 local minima (index 1). Using gradient ascent from the local minima, this yields 6 connected components, 2 with a single local maximum and local minimum and 4 with two local maxima and local minima, confirming the results in [23, Ex. 6.4].

To justify our choice of ϵ, we also considered the system where ϵ was a free parameter and computed the discriminant with respect to ϵ. This computation showed that the smallest positive root of the discriminant with respect to ϵ to be approximately 0.01438729081. Hence, for any $\epsilon > 0$ less than this value, the structure of the routing points will be the same yielding an octic curve with the same real geometry. In particular, this justifies our choice of $\epsilon = 10^{-2}$ as it is smaller than the smallest positive root of the discriminant.

6.4 Counting input modes for a five-bar mechanism

Input modes of a five-bar mechanism, which is illustrated in Figure 7 with more details provided in [16, Fig. 2], are the connected components of the corresponding configuration space after removing the input singularities [16]. There are transmission problems at input singularities causing a loss of control authority of the end-effector. Hence, in [16], a margin around the input singularities was avoided, which may be for the application to provide a safety margin, e.g., to accommodate manufacturing tolerances. Nonetheless, the following considers computing the actual number of input modes without the safety margin.

Adapted from [16], the configuration space is defined by $g = \{g_1, \ldots, g_4\} = 0$ with parameters $(b_x, \ell_1, \ell_2, \ell_3, \ell_4, p, q)$ and variables $(x, y, c_1, s_1, c_2, s_2)$ where $c_j = \cos\theta_j$ and $s_j = \sin\theta_j$, such that

$$
\begin{aligned}
g_1 &= x^2 + y^2 + \ell_1^2 - 2\ell_1(xc_1 + ys_1) - p^2 - q^2, \\
g_2 &= \ell_2^2(x^2 + y^2) + \ell_1^2((\ell_2 - p)^2 + q^2) + (bx^2 + \ell_3^2 - \ell_4^2)(p^2 + q^2) - 2b_x\ell_2(px + qy) \\
&\quad - 2\ell_2\ell_3(p(xc_2 + ys_2) - q(xs_2 - yc_2)) + 2\ell_1\ell_3((\ell_2 p - p^2 - q^2)(c_1c_2 + s_1s_2)) \\
&\quad + 2b_x\ell_3(p^2 + q^2)c_2 + 2b_x\ell_1((\ell_2 p - p^2 - q^2)c_1 + \ell_2 q s_1) - 2\ell_1\ell_2\ell_3 q(c_1s_2 - s_1c_2) \\
&\quad + 2\ell_1\ell_2((p - \ell_2)(xc_1 + ys_1) - q(xs_1 - yc_1)), \\
g_3 &= c_1^2 + s_1^2 - 1, \\
g_4 &= c_2^2 + s_2^2 - 1.
\end{aligned}
$$

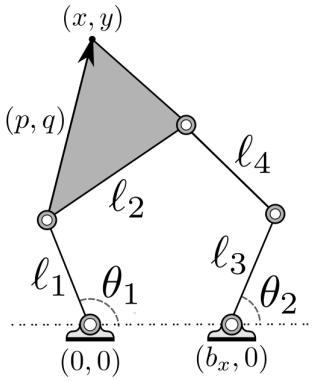

Figure 7: Illustration of a five-bar mechanism

The input singularities are defined by

$$f = \det \begin{bmatrix} \frac{\partial g_1}{\partial x} & \frac{\partial g_1}{\partial y} \\ \frac{\partial g_2}{\partial x} & \frac{\partial g_2}{\partial y} \end{bmatrix} = 0.$$

For the parameters, corresponding with [16, Ex. 1],

$$\begin{array}{rclcrcl} b_x &=& 0.19882665671846764, & & \ell_1 &=& 0.46540235567944005, \\ p &=& 0.048759206368821334, & & \ell_2 &=& 0.3486213752206714, \\ q &=& 0.32778886030888477, & & \ell_3 &=& 0.24863642973175545, \\ & & & & \ell_4 &=& 0.4110712177344681, \end{array}$$

$X = V_{\mathbb{R}}(g)$ is a smooth surface in $\mathbb{R}^6$ and f is a quadratic polynomial such that $\{g, f\} = 0$ defines two irreducible curves of degree 6 in $\mathbb{C}^6$. Using the routing function

$$r = \frac{f}{((x-x_0)^2 + (y-y_0)^2 + (c_1-c_{10})^2 + (s_1-s_{10})^2 + (c_2-c_{20})^2 + (s_2-s_{20})^2 + 1)^2}$$

where

$$\begin{array}{rclcrclcrcl} x_0 &=& 0.919487917032162, & & y_0 &=& -0.319228546667734, & & c_{10} &=& 0.170535501959555, \\ s_{10} &=& 0.502534118611306, & & c_{20} &=& -0.552376121017726, & & s_{20} &=& -0.489809769081462, \end{array}$$

were randomly selected, there are 8 routing points: four each with $f > 0$ and $f < 0$. For $f > 0$, there is a maximum and three saddles of index 1. For $f < 0$, there is a minimum and three saddles of index 1. Hence, Proposition 3.2 immediately yields that X_r has two smoothly connected components, one with $f > 0$ and the other with $f < 0$. When partitioning with a "thicker kerf," [16] reports 6 input modes with the comment that the "counts generally do not match the true number of regions" due to the safety margin around the input singularities.

7 Conclusion

By using gradient ascent/descent paths on a real algebraic variety, algorithms were developed for computing the Euler characteristic, counting the number of smoothly connected components, and performing membership in a smoothly connected component. In particular, Algorithm 1 computes a representation of each smoothly connected component consisting of routing points and gradient ascent/descent paths which can be used to decide membership via Algorithm 2. Such algorithms could naturally be extended to atomic semi-algebraic sets, with an example presented for considering the intersection of a real algebraic variety with the positive orthant.

As constructed, the algorithms rely upon the ability to construct a routing function, which relies upon a generic choice of a constant vector c. An element of more concern when implementing such a theoretical algorithm is is the proper tracking of gradient ascent/descent paths emanating from unstable eigenvector directions. Future work could be to investigate using certified differential equation solvers for validating the numerically computed trajectories.

Acknowledgment

J.C. and J.D.H. thank Liviu Nicolaescu for discussions involving Morse theory and corresponding book. All authors thank the anonymous reviewer for suggestions to improve the manuscript.

Author contribution

All authors contributed to the writing of the main manuscript text and reviewed the manuscript.

Funding

J.D.H. was supported in part by National Science Foundation grant CCF 2331400, Simons Foundation SFM-00005696, and the Robert and Sara Lumpkins Collegiate Professorship. H.H. was supported in part by National Science Foundation grants CCF 2331401 and CCF 2212461. C.S. was supported in part by Simons Foundation grant 965262.

Data availability

All data is described in the text.

Ethical approval

Not applicable.

Conflict of interest

The authors declare no competing interests.

References

[1] A. Ambrosetti. Elliptic equations with jumping nonlinearities. *J. Math. Phys. Sci.*, 18(1):1–12, 1984.

[2] A. Banyaga and D. Hurtubise. *Lectures on Morse homology*, volume 29 of *Kluwer Texts in the Mathematical Sciences*. Kluwer Academic Publishers Group, Dordrecht, 2004.

[3] S. Basu, R. Pollack, and M.-F. Roy. Computing roadmaps of semi-algebraic sets on a variety. *J. Amer. Math. Soc.*, 13(1):55–82, 2000.

[4] S. Basu, R. Pollack, and M.-F. Roy. *Algorithms in real algebraic geometry*, volume 10 of *Algorithms and Computation in Mathematics*. Springer-Verlag, Berlin, second edition, 2006.

[5] S. Basu and M.-F. Roy. Divide and conquer roadmap for algebraic sets. *Discrete Comput. Geom.*, 52(2):278–343, 2014.

[6] S. Basu, M.-F. Roy, M. Safey El Din, and E. Schost. A baby step–giant step roadmap algorithm for general algebraic sets. *Found. Comput. Math.*, 14(6):1117–1172, 2014.

[7] D. J. Bates, J. D. Hauenstein, C. Peterson, and A. J. Sommese. Numerical decomposition of the rank-deficiency set of a matrix of multivariate polynomials. In L. Robbiano and J. Abbott, editors, *Approximate Commutative Algebra*, pages 55–77. Springer Vienna, Vienna, 2010.

[8] D. J. Bates, J. D. Hauenstein, A. J. Sommese, and C. W. Wampler. Bertini: Software for numerical algebraic geometry. Available at bertini.nd.edu with permanent doi: dx.doi.org/10.7274/R0H41PB5, 2006.

[9] E. Becker and R. Neuhaus. Computation of real radicals of polynomial ideals. In *Computational algebraic geometry (Nice, 1992)*, volume 109 of *Progr. Math.*, pages 1–20. Birkhäuser Boston, Boston, MA, 1993.

[10] O. Bohigas, M. E. Henderson, L. Ros, and J. M. Porta. A singularity-free path planner for closed-chain manipulators. In *2012 IEEE International Conference on Robotics and Automation*, pages 2128–2134, 2012.

[11] O. Bohigas, M. Manubens, and L. Ros. *Singularities of Robot Mechanisms: Numerical Computation and Avoidance Path Planning*, volume 41 of *Mechanisms and Machine Science*. Springer, [Cham], 2017.

[12] D. A. Brake, J. D. Hauenstein, and C. Vinzant. Computing complex and real tropical curves using monodromy. *J. Pure Appl. Algebra*, 223(12):5232–5250, 2019.

[13] J. Canny. *The complexity of robot motion planning*, volume 1987 of *ACM Doctoral Dissertation Awards*. MIT Press, Cambridge, MA, 1988.

[14] J. Canny. Computing roadmaps of general semi-algebraic sets. *Comput. J.*, 36(5):504–514, 1993.

[15] J. Canny, D. Y. Grigor'ev, and N. N. Vorobjov, Jr. Finding connected components of a semialgebraic set in subexponential time. *Appl. Algebra Engrg. Comm. Comput.*, 2(4):217–238, 1992.

[16] P. B. Edwards, A. Baskar, C. Hills, M. Plecnik, and J. D. Hauenstein. Output mode switching for parallel five-bar manipulators using a graph-based path planner. In *2023 IEEE International Conference on Robotics and Automation (ICRA)*, pages 9735–9741, 2023.

[17] D. Y. Grigor'ev and N. N. Vorobjov, Jr. Counting connected components of a semialgebraic set in subexponential time. *Comput. Complexity*, 2(2):133–186, 1992.

[18] J. Heintz, M.-F. Roy, and P. Solernó. Single exponential path finding in semialgebraic sets. I. The case of a regular bounded hypersurface. In *Applied algebra, algebraic algorithms and error-correcting codes (Tokyo, 1990)*, volume 508 of *Lecture Notes in Comput. Sci.*, pages 180–196. Springer, Berlin, 1991.

[19] J. Heintz, M.-F. Roy, and P. Solernó. Single exponential path finding in semi-algebraic sets. II. The general case. In *Algebraic geometry and its applications (West Lafayette, IN, 1990)*, pages 449–465. Springer, New York, 1994.

[20] H. Hong. Connectivity in semi-algebraic sets. In T. Ida, V. Negru, T. Jebelean, D. Petcu, S. M. Watt, and D. Zaharie, editors, *12th International Symposium on Symbolic and Numeric Algorithms for Scientific Computing, SYNASC 2010, Timisoara, Romania, 23-26 September 2010*, pages 4–7. IEEE Computer Society, 2010.

[21] H. Hong, J. Rohal, M. Safey El Din, and E. Schost. Connectivity in semi-algebraic sets I. arXiv:2011.02162, 2020.

[22] D. Kincaid and W. Cheney. *Numerical Analysis: Mathematics of Scientific Computing*. Brooks/Cole Publishing Co., Pacific Grove, CA, third edition, 2002.

[23] M. Kummer, B. Sturmfels, and R. Vlad. Maximal Mumford curves from planar graphs. arXiv:2404.11838, 2024.

[24] D. G. Luenberger. The gradient projection method along geodesics. *Management Science*, 18(11):620–631, 1972.

[25] J. J. Moré and T. S. Munson. Computing mountain passes and transition states. *Math. Program.*, 100(1):151–182, 2004.

[26] L. Nicolaescu. *An Invitation to Morse Theory*. Universitext. Springer, New York, second edition, 2011.

[27] J. T. Schwartz, M. Sharir, and J. Hopcroft, editors. *Planning, Geometry, and Complexity of Robot Motion*. Ablex Series in Artificial Intelligence. Ablex Publishing Corporation, Norwood, NJ, 1987.

[28] A. J. Sommese and C. W. Wampler, II. *The Numerical Solution of Systems of Polynomials Arising in Engineering and Science*. World Scientific Publishing Co. Pte. Ltd., Hackensack, NJ, 2005.

[29] Y. Yang. Globally convergent optimization algorithms on Riemannian manifolds: uniform framework for unconstrained and constrained optimization. *J. Optim. Theory Appl.*, 132(2):245–265, 2007.